## 3.2.7 The phylogeny of *Serica*

*Serica* is with more than a hundred species one of the most diverse sericine genera in the Palearctic region, known to occur in the temperate regions of Eurasia and the higher mountains of Asia, only. All species occur in forest habitats, from 400 to over 4300 meters, but specialized high altitude specialists have not evolved. The taxonomy and distribution of the Himalayan species of the genus have been revised recently (Ahrens 1999c), while the taxa of the Asian mainland are reviewed in Ahrens (in press c). A complete checklist of the taxa so far assigned to *Serica* including synonymy is in preparation in the framework of the furthcoming catalogue of Palearctic Coleoptera.

### Material and methods

*Taxon sampling and characters*

One hundred and twenty-three species belonging to eight genera were included in the cladistic analysis. One taxon, *Pleophylla* sp., was chosen as outgroup taxon due to its rather close relationship to the ingroup taxa but being with high probability not part of the ingroup (chapter 3.1). The choice of the taxa composing the ingroup was mainly based on modern classification of the *Serica* species (Nomura 1972; Ahrens 1999c). To test monophyly of *Serica* and to explore, preliminarily, the relationships of *Serica* to other groups, representatives of several other genera of Sericini were included. These taxa were mainly selected based on some presumptive apomorphies which they are hypothesized to share with *Serica* (Ahrens 2003c, in press b, and unpublished results).

Character coding was based on 129 species belonging to nine genera (see appendix A 3.2.7). The description of the new species as well as material studied for this analysis is referred in Ahrens (in press c). Hundred and fifteen adult characters were scored here. The character states are illustrated in Figs 91-96.

*Phylogenetic analysis*

The 117 characters (68 binary and 49 multistate) were all unordered and equally weighted. Inapplicable characters were coded as "-", while missing character states were coded as "?" (Strong and Lipscomb 1999). The parsimony analysis was performed in NONA 2.0 (Goloboff 1999) using the parsimony ratchet (Nixon 1999) implemented in NONA, run with WINCLADA vs. 1.00.08 (Nixon 2002) as a shell program. Two hundred iterations were performed (one tree held per iteration), the search was repeated ten times. The number of characters to be sampled for reweighting during the parsimony ratchet was determined to be 11. All searches were done under the collapsing option "ambiguous" which collapses every node with a minimum length of 0.

Bremer support (Bremer 1988, 1994) and bootstrap values (Felsenstein 1985) were evaluated using NONA. Bootstrap analyses of data were performed with 1000 replicates using TBR branch swapping. The search was set to a Bremer support level of 12 (based on the number of unambiguous character changes for each node given by WINCLADA), with seven runs (each holding a number of trees from 100 to 500 times multiple of suboptimal tree length augmentation) and a total hold of 8000 trees. Character changes were studied and mapped on the tree using WINCLADA.

Successive weighting (Farris 1969) was used to further evaluate phylogenetic relationships. This method uses *post hoc* character weighting based on the fit of each character as applied to the trees currently in memory. Thus, the 'quality' of the character data is used rather than intuitive feeling regarding weighting of characters. Although this method increases the assumptions in the analysis (Siebert 1992), it is useful for analysing

phylogenetic pattern when characters exhibit a high level of homoplasy. Characters were reweighted based on the consistency index, retention index, and the rescaled consistency index (Farris 1989). The base weight was set at 100. Weights were inserted into NONA parsimony ratchet search via the WINCLADA surface manually. Tree searches continued until the character weights no longer changed (Farris 1988) or until identical trees were found in consecutive searches (indicating stability in the trees).

## Characters and character states

In describing character states, I refrain from formulating any hypothesis about their transformation. In particular, coding does not imply whether a state is derived or ancestral. The data matrix is presented in the appendix B 3.2.7.

*Integument*

1. *Body, dorsal face*: (0) dull, with tomentum made of minute trichomes (Figs 91B,C); (1) simply shiny, without tomentum (Fig. 91A); (2) shiny, with small patches of tomentum.
2. *Body, colouration of dorsal face* (0) multicoloured (Figs 91B,C); (1) monochrome (Fig. 91A).

*Head*

3. *Labrum anteriorly beside median sinuation*: (0) not toothed (Figs 91E,F, black arrow, H,M,N); (1) toothed (Fig. 91D, black arrow).
4. *Labrum ventrally*: (0) not widened vertically (Fig. 91M); (1) widened vertically (Fig. 91D); (2) widened vertically, but strongly concave ventroapically (Fig. 91N).
5. *Labroclypeus, anterior margin medially*: (0) weakly sinuate (Figs 91D, white arrow, M,N); (1) deeply sinuate (Fig. 91E, white arrow); (2) not sinuate (Fig. 91F, white arrow).
6. *Labroclypeus, lateral margins*: (0) weakly reflexed; (1) strongly reflexed.
7. *Labroclypeus, lateral margins*: (0) weakly convex (Figs 91D,H); (1) strongly convex (Figs 91E,J).
8. *Labroclypeus, basis*: (0) shiny, without tomentum (Figs 91D-F); (1) dull, with tomentum (Fig. 91H).
9. *Frons behind frontoclypeal suture*: (0) plane (Figs 91D-F,H); (1) impressed (Fig. 91J, arrow).
10. *Frons in male*: (0) completely dull (Figs 91D,H,K); (1) completely shiny (Figs 91F,E); (2) shiny, posteriorly dull only (Fig. 91J); (3) 0&2.
11. *Head behind eyes*: (0) short (Figs 91G,L,O-Q); (1) long (Fig. 91K).
12. *Postocular groove*: (0) present (Figs 91G,L); (1) absent (Fig. 91K).
13. *Labium anteriorly*: (0) convex (Fig. 91M, white arrow); (1) flat; (2) flat and longitudinally impressed; (3) weakly convex, apically concave (Fig. 91N, white arrow).
14. *Angle of galea in relation to axis of maxilla*: (0) ~ 90° or smaller (Figs 91S-U,W,X); (1) > 90° (Fig. 91V).
15. *Maxilla*: (0) with four visible teeth ventrally (Figs 91S-V,X); (1) with three visible teeth ventrally (Fig. 91W).
16. *Antenna, number of antennomeres*: (0) ten; (1) nine; (2) 0&1.
17. *Antennal club in male, number of antennomeres*: (0) four; (1) three; (2) six.
18. *Antennal club in male, in relation to remainder of antennomeres*: (0) as long or little longer (at maximum 1,5 times) (Fig. 91C); (1) at least twice as long (Figs 91A,B).

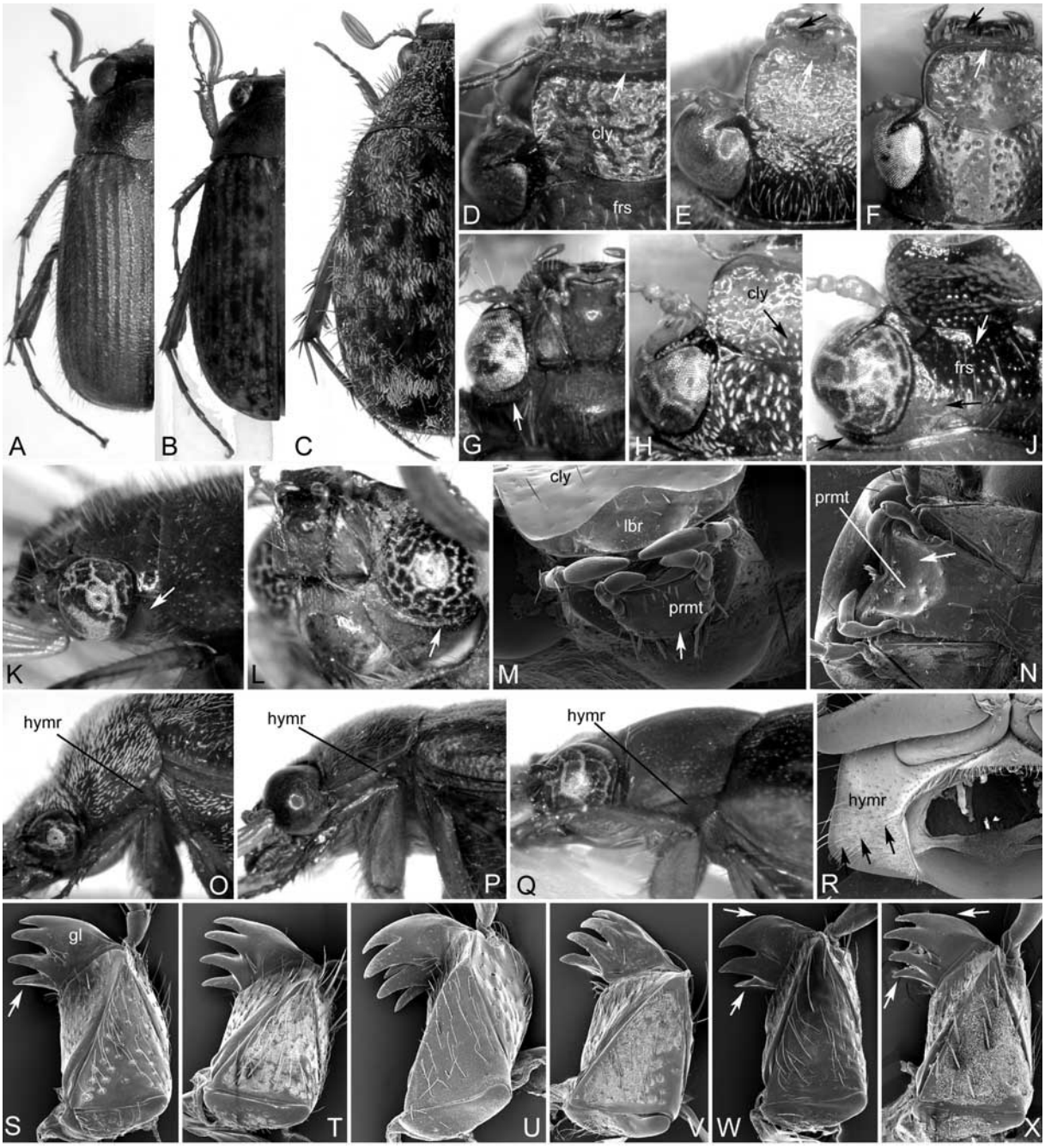


**Fig. 91. A, E, P:** *Serica fulvopubens*; **B, J, Q:** *S. shaanxiensis*; **C, S:** *Pachyserica olafi*; **D:** *P. rubrobasalis*; **F:** *Gastroserica asulcata*; **G:** *Lasioserica maculata jiriana*; **H:** *S. nigroguttata*; **K, V:** *Calloserica langtangica*; **M, X:** *S. thibetana*; **N, R:** *S. kingdoni*; **O:** *S. inaequalis*; **T:** *L. modikholae*; **U:** *G. marginalis*; **W:** *S. heydeni*. **A-C:** Body, left half in dorsal view; **D-F, H, J:** head, dorsal view; **G, L, N:** head ventral view; **K:** head, lateral view; **M:** head, cranial view; **O-Q:** head + prothorax, lateral view; **R:** prothorax, ventral view; **S-X:** right maxilla, ventral view (not to scale).

*Thorax*

19. *Hypomeron ventrally*: (0) not edged (Figs 91R, black arrows, 91P,Q); (1) edged (Fig. 91O); (2) 0&1.
20. *Pronotum, anterior angles*: (0) distinctly produced and sharp; (1) weakly produced and moderately rounded; (2) not produced and strongly rounded.
21. *Pronotum, anterior marginal line medially*: (0) complete; (1) widely interrupted.
22. *Pronotum, posterior angles*: (0) sharp or blunt; (1) strongly rounded.
23. *Pronotum, longer pilosity on disc*: (0) directed posteriorly (Fig. 91P); (1) directed anteriorly (Fig. 91K); (2) absent (Fig. 91Q); (3) 0&2.

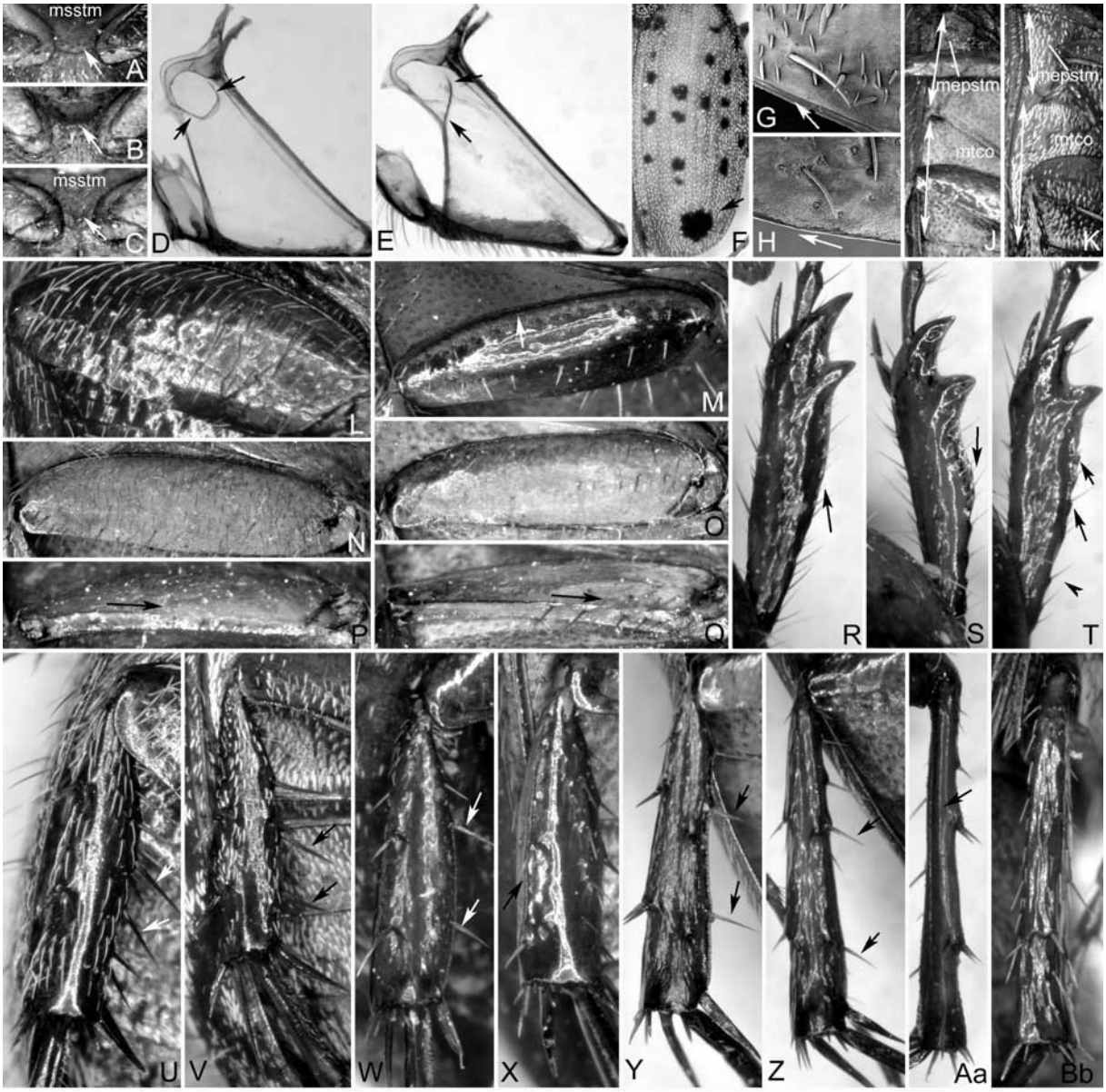


**Fig. 92. A, G, K, V:** *Pachyserica olafi*; **B, D, F:** *Serica nigroguttata*; **C, E, O, P, Y:** *S. khasiana*; **H:** *S. thibetana*; **J, Q, Z:** *S. pommeranzi*; **L, U:** *Pleophylla* sp.; **M, X:** *Lasioserica modikholae*; **N:** *Calloserica langtangica*; **R:** *S. kingdoni*, **S:** *S. yulongshanica*; **T:** *S. furcata*; **W:** *S. inaequalis*; **Aa:** *S. weiperti*; **Bb:** *S. montreuili*. **A-C:** meso- and metasternum between mesocoxae, ventral view; **D, E:** metafurca, lateral view; F: elytra, dorsal view; **G, H:** apical margin of elytra, caudal view; **J, K:** metepisternum and metacoxa, ventrolateral view; **L-Q:** metafemur, ventral view; **R-T:** protibia, dorsal view; **U-Z:** metatibia, lateral view; **Aa, Bb:** metatibia, dorsal view (not to scale).

24. *Pronotum, shorter pilosity on disc*: (0) absent; (1) present (Figs 91K,O-Q).
25. *Mesosternum, setae between mesocoxae*: (0) evenly dispersed (Fig. 92C); (1) on a semicircular carina (Figs 92A,B).
26. *Metasternum anteriorly*: (0) evenly elevated; (1) abruptly and strongly elevated.
27. *Elytra*: (0) with dark or light spots (Figs 91B, 92F); (1) uniformly yellowish brown (Fig. 91A); (2) uniformly reddish brown; (3) uniformly black.
28. *Elytra, a large dark spot before apex*: (0) absent (Figs 91A-C); (1) present (Fig. 92F)
29. *Elytra, long pilosity*: (0) thin, seta-like (Fig. 91P); (1) thick, seta-like (Fig. 91O); (2) scale-like (Figs 91C, 92F); (3) thin and thick, seta-like.
30. *Elytra, long pilosity*: (0) on all intervals throughout entire surface; (1) on odd intervals exclusively; (2) on sutural interval exclusively; (3) on base exclusively; (4) on base, sides and apical declivity.

31. *Elytra, short pilosity*: (0) thinly seta-like and long (Fig. 91P); (1) thickly seta-like and short (Fig. 91Q); (2) reduced (or minute; 100 x magnification); (3) largely scale-like (Fig. 91C); (4) largely scale-like and thickly seta-like.
32. *Elytra, short pilosity*: (0) slightly erect but bent posteriorly; (1) strongly adpressed; (2) erect and adpressed (0&1).
33. *Elytra, short pilosity*: (0) dense, setae separated by much less than one length of a seta (Figs 91A,P); (1) sparse, setae separated by more than one length of a seta (Figs 91B,Q).
34. *Elytra, microtrichomes on apical margin*: (0) present (Fig. 92G); (1) absent (Fig. 92H); (2) 0&1.
35. *Body, pilosity of ventral face*: (0) setose (Figs 91P, 92J); (1) scale-like, at least partly (Figs 91O, 92K).
36. *Metafurca, lateral lamina posteriorly*: (0) curved dorsally (Fig. 92D, upper arrow); (1) almost straight (Fig. 92E, upper arrow).
37. *Metafurca, lateral lamina anteriorly*: (0) curved dorsally (Fig. 92D, lower arrow); (1) straight directed ventrally (Fig. 92E, lower arrow); (2) shortened, not reaching the anterior lamina.

*Legs*

38. *Metacoxa (ratio of length of metepisternum/ length of metacoxa)*: (0) not enlarged (1/1.2-1.6) (Fig. 92J); (1) enlarged (1/ >1,7) (Fig. 92K).
39. *Metacoxa on lateral half shortly behind middle*: (0) not impressed; (1) impressed.
40. *Metacoxa ventrally*: (0) glabrous except a few setae laterally (Figs 92J,M); (1) all punctures setose (with setae or scales) (Figs 92K,L).
41. *Metafemur ventrally*: (0) between the two longitudinal rows of setae densely setaceous (Figs 92L,N); (1) between the two longitudinal rows of setae glabrous or very sparsely setose (Figs 92M,O-Q).
42. *Metafemur, posterior ventral margin apically*: (0) not serrate (Figs 92L,M, 93D); (1) serrate (Figs 92O-Q).
43. *Metafemur, posterior dorsal margin apically*: (0) not serrate; (1) serrate (Figs 92P,Q).
44. *Metafemur, posterior marginal edge on ventral side begins*: (0) behind basal quarter of metafemur (Fig. 92P); (1) behind basal half of metafemur (Fig. 92Q).
45. *Metafemur, submarginal serrated line beside anterior margin*: (0) absent; (1) present.
46. *Protibia*: (0) long (more than four times as long as wide) (Figs 92R-T); (1) short (maximally three times as long as wide) (Ahrens in press c).
47. *Protibia, external lateral margin medially*: (0) straight (Fig. 92R); (1) bluntly widened (Fig. 92S).
48. *Protibia, external lateral margin*: (0) smooth (Figs 92R,S); (1) finely toothed (Fig. 92T).
49. *Mesotibia, apical spur*: (0) straight; (1) curved ventrally.
50. *Metatibia (ratio of length/ width)*: (0) short (1/ 3.9-4.4) (Figs 92U-X); (1) long (1/ > 4,6) (Figs 92Y,Z).
51. *Metatibia, apex interiorly near tarsal articulation*: (0) weakly truncate (less deep than wide) (Figs 93A,B); (1) sharply truncate (as deep as wide or deeper than wide) (Fig. 92C).
52. *Metatibia, setae of ventral margin*: (0) robust (their longitudinal grooves visible with 100x magnification; compare to small apical spines of metatibia (Fig. 93E)); (1) fine (their longitudinal grooves invisible with 100x magnification).
53. *Metatibia, setae of ventral margin*: (0) weakly separate (the two apical setae in apical half of metatibia) (Figs 92U,V); (1) widely separate (the two apical setae in apical two thirds of metatibia) (Figs 92W,Y,Z); (2) 0&1.
54. *Metatibia, dorsal margin*: (0) sharply edged (Figs 92V-Z); (1) longitudinally convex (Figs 92U,Aa,Bb).

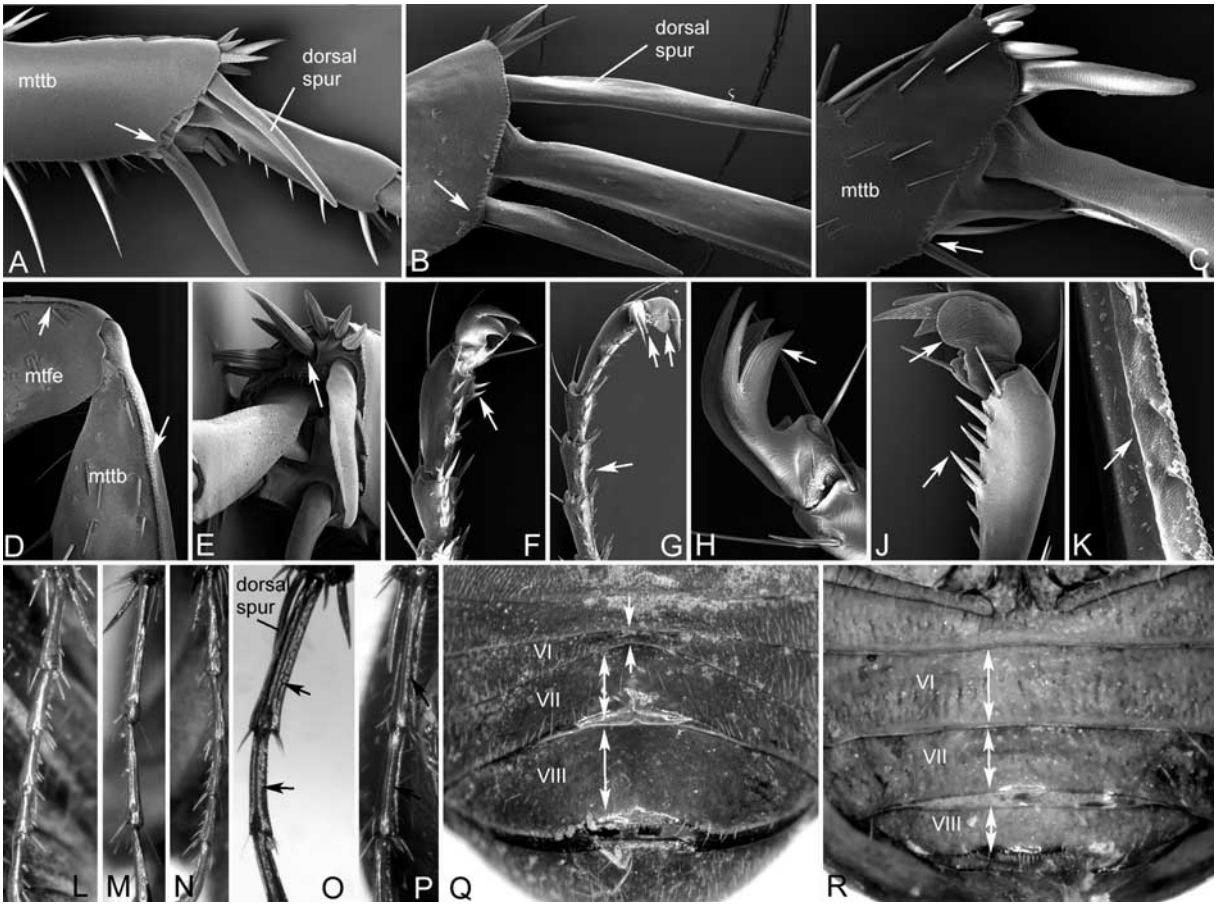


**Fig. 93. A, E:** *Pleophylla* sp.**, B, H, J, O:** *Serica thibetana*; **C:** *Amiserica krausei*; **D:** *Lasioserica modikholae*; **F, G:** *S. tukucheana*; **K:** *S. nepalensis*; **L:** *S. montreuili*; **M, P:** *S. kingdoni*; **N:** *S. shaanxiensis*; **Q:** *S. bailungshanica*; **R:** *S. khasiana.* **A-C:** apex of metatibia, medial view; **D:** metafemur and metatibia, ventrolateral view; **E:** apex of metatibia, caudal view; **F-J:** protarsal claws, medial view; **K:** metatarsomere 1, ventral view; **L-M:** mesotarsomeres, lateral view; **O, P:** metatarsomeres, lateral view; **Q, R:** abdominal sternites, ventral view (not to scale).

55. *Metatibia, longitudinal serrated line on dorsolateral face*: (0) completely absent (Figs 92U-W,Y-Bb); (1) present throughout basal three quarter of metatibial length (Fig. 92X); (2) present throughout in basal half of metatibial length.
56. *Metatibia, interior spines on apical face*: (0) present (Fig. 93E); (1) absent (chapter 3.1).
57. *Metatibia, pilosity of lateral face composed of*: (0) fine setae (Fig. 92U); (1) scales (and fine setae) (Fig. 92V); (2) absent (Figs 92W-Z).
58. *Metatibia, basal third dorsolaterally*: (0) longitudinally convex (Figs 92U,Aa,Bb); (1) weakly carinate (Figs 92V-Y).
59. *Protarsomere V, setae ventrally*: (0) fine (Fig. 93G); (1) robust and short (Fig. 93F).
60. *Protarsomere V, ratio (r) of length/ width*: (0) $2.9 \leq r < 3.3$; (1) $2.5 \leq r < 2.9$; (2) $r < 2.5$; (3) $3.3 \leq r < 3.9$; (4) $3.9 \leq r < 4.6$; (5) $r \geq 4.6$.
61. *Protarsal claw, basal tooth of interior claw*: (0) sharply pointed, similar to the basal tooth of the meso- and metatarsal claw (Figs 93F,H); (1) lobiform (Fig. 93J); (2) s-shaped curved and sharply pointed ventrally; (3) completely absent; (4) bluntly truncate.
62. *Protarsal claw, basal tooth of external claw*: (0) sharply pointed, similar to the basal tooth of the meso- and metatarsal claw (Fig. 93H); (1) lobiform (Fig. 93G); (2) bluntly truncate.
63. *Ratio length of elytra/ length of all mesotarsomeres combined*: (0) $r \geq 2.5$; (1) $2.25 \leq r < 2.5$; (2) $2{,}0 < r < 2{,}25$; (3) $1.6 < r \leq 2.0$; (4) $r \leq 1.6$.
64. *Mesotarsomeres dorsally*: (0) smooth, impunctate (Figs 93L,M); (1) punctate; (2) longitudinally wrinkled (Fig. 93N); (3) 0&1.

65. *Mesotarsomeres laterally*: (0) not carinate (Fig. 93L); (1) carinate (Figs 93M,N).
66. *Metatarsomeres laterally*: (0) not carinate; (1) carinate (Figs 93O,P).
67. *Metatarsomere I, supplementary ventrolateral carina beside serrated ventral carina*: (0) robust, visible with 50 x magnification (Fig. 93P); (1) very fine or completely absent (Figs 93K,O); (2) fused with ventral carina.
68. *Metatarsomere I*: (0) little longer than the dorsal metatibial spur (Figs 93A,P); (1) about twice as long as the dorsal metatibial spur (Fig. 93O).
69. *Metatarsomeres, apical setae*: (0) short and robust (at maximum one quarter of the length of the subsequent tarsomere); (1) long (~ one third of the length of the subsequent tarsomere).

*Abdomen*

70. *Abdomen, pilosity except for transverse rows of robust setae*: (0) dense (Fig. 93Q); (1) sparse (Fig. 93R).
71. Sixths abdominal sternite medially: (0) as long as the preceding sternite (Fig. 93R); (1) strongly shortened, half as long as the preceding sternite (Fig. 93Q).
72. *Abdomen, last abdominal sternite*: (0) shorter or of the same length as preceding sternite (Fig. 93R); (1) longer than the preceding sternite (Fig. 93Q).
73. *Abdomen, penultimate abdominal sternite*: (0) flat, not elevate (Figs 93Q,R); (1) transversely elevate medially; (2) bituberculate.

*Male genitalia*

74. *Phallobase, at middle ventroapically*: (0) concavely sinuate (Fig. 94A); (1) produced (Fig. 94B).
75. *Phallobase, at middle dorsoapically*: (0) concavely sinuate (Figs 94C,E); (1) median sinuation in parts sclerotized and medially produced triangularly (Fig. 94F); (2) diagonally truncate, between insertion of parameres with an evenly straight margin (Fig. 94E).
76. *Phallobase, median sinuation (dorsal view)*: (0) shallow (Fig. 94C); (1) deep (Fig. 94D); (2) strongly asymmetric, with sinuation left side shallow and right side deep (Figs 95C,T).
77. *Phallobase, before apex ventrally*: (0) without tubercles (Figs 94A,B); (1) with convex elevation (Figs 95F,O); (2) with two tubercles.
78. *Phallobase, before apex dorsally*: (0) without tubercles (Figs 94C-F); (1) with two tubercles (Figs 95B,E,F, arrow).
79. *Phallobase, insertion of left paramere*: (0) at the same level as the left one (Figs 95A,B,E,L,U); (1) weakly displaced basally (Figs 95J,Q,S); (2) strongly displaced basally (by more than maximal distal width of phallobase) (Fig. 95C); (3) displaced apically (Fig. 95K).
80. *Parameres*: (0) not subdivided into a long dorsal and ventral lobe, or only one of both subdivided into a long dorsal and ventral lobe; (1) both subdivided into a long dorsal and ventral lobe (Figs 94K, white arrows, 95L, arrows).
81. *Parameres (lateral view)*: (0) both straight (Figs 95D,G); (1) both curved ventrally at middle (Figs 95H,O); (2) apex of the right paramere curved ventrally (Fig. 95M); (3) right paramere curved ventrally at middle (Figs 95F, 96B); (4) curved dorsally at middle (Fig. 95N).
82. *Parameres*: (0) equal in length (Figs 95A,B,L,P,Q); (1) left paramere moderately shortened (Figs 95C,E,J,K,R,S,U-W,Z,Aa-Dd,Ff-Hh); (2) left paramere strongly shortened (more than half as long than the right paramere) (Figs 95D,T,Bb,Ee).
83. *Right paramere, narrow basal lobe directed medially*: (0) absent (Figs 95A-C,E,J,K,P-U,W,Z-Hh); (1) present (Figs 94K, 95L,V).

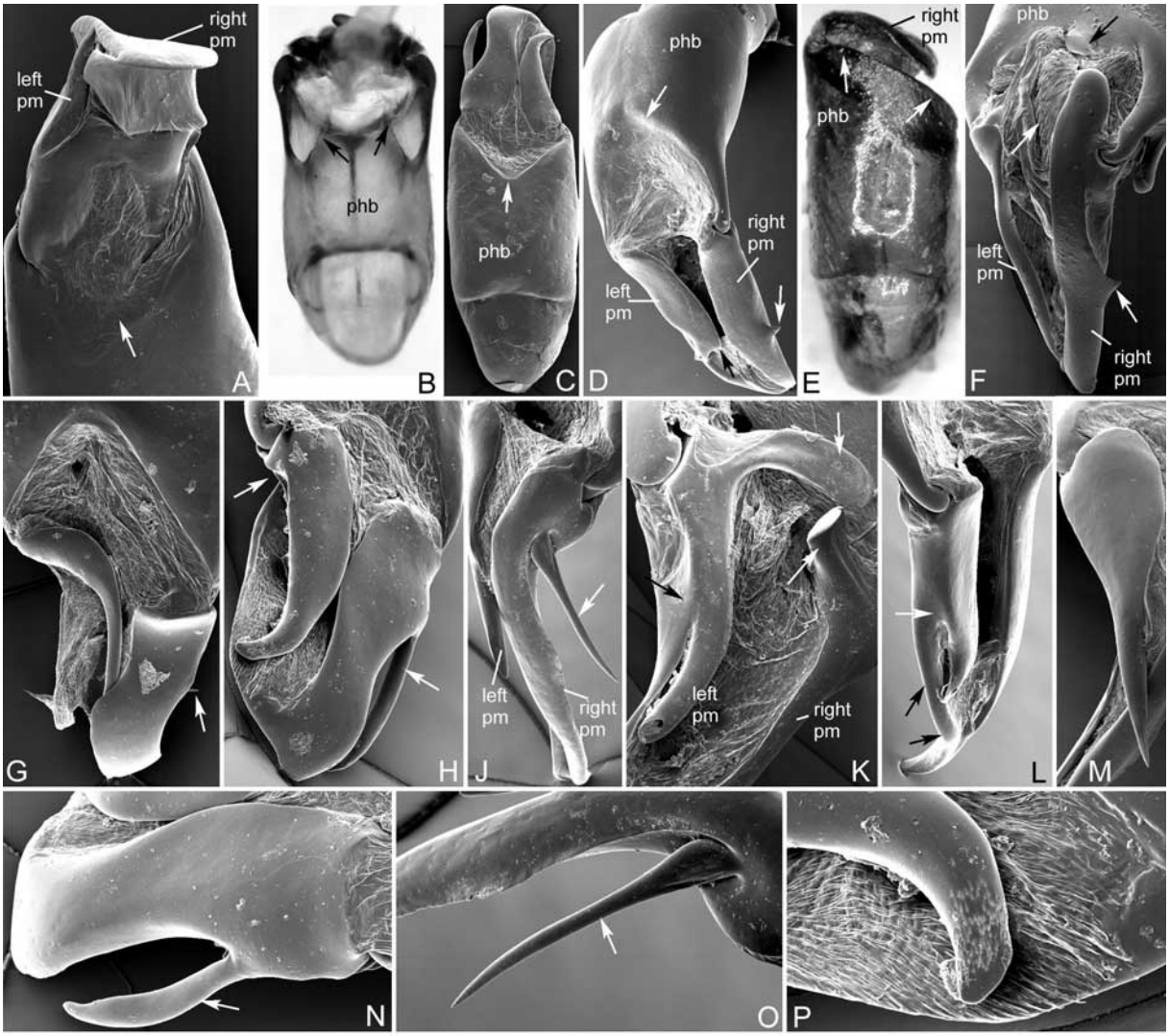


**Fig. 94. A:** *Serica pommeranzi*; **B:** *Amiserica krausei*; **C, H, N, P:** *S. ramosa*; **D, L:** *S. shaanxiensis*; **E:** *S. nanjangana*; **F:** *S. inaequalis*; **G:** *S. nepalensis*; **J, M, O:** *S. tukucheana*; **K:** *S. heydeni*. **A, B:** aedeagus, ventral view; **C, E:** aedeagus, dorsal view; **D:** aedeagus, dorsolateral view; **F-K:** parameres, dorsal view; **L, M:** left paramere, left side dorsolateral view; **N, O:** right paramere, right side dorsolateral view; **P:** left paramere, dorsal view (not to scale).

84. *Right paramere*: (0) distinctly protruding insertion of medial membrane (Figs 95B,C, E,L,Q,R,Bb,Dd,Ff-Hh); (1) not protruding insertion of medial membrane (Figs 95J,P, S,T,Aa,Cc,Ee).
85. *Right paramere, in cross section*: (0) dorsoventral extension and mediolateral extension equal (Figs 95A,M,K,N,E,F); (1) mediolateral extension distinctly greater than dorsoventral extension (Figs 95X,Y,Z,Aa).
86. *Right paramere apically (dorsal view)*: (0) straight (Figs 95A,L,R,V,Aa,Ee-Hh); (1) curved (directed) medially (inward) (Figs 95J,W); (2) curved (directed) laterally (outward) (Figs 95B,C,E,R).
87. *Right paramere in basal three quarter*: (0) narrowed distally (Figs 95A-C,E,J,R,Cc); (1) subequal in width (Figs 95P,Q,T,Aa,Ee); (2) widened distally (Figs 95Z,Bb).
88. *Right paramere apically* (0) not widened (Figs 95A-C,E,J,P,R,Cc); (1) widened interiorly (Figs 95Aa,Bb); (2) widened laterally (Fig. 95Dd); (3) widened interiorly and laterally (Fig. 95Z).
89. *Right paramere, lateral preapical tooth*: (0) absent (Figs 94G,H, 95A-C,E,K,L,R-W,Aa-Dd); (1) present (Figs 94D,F, 95J,P,Q,Ff-Hh).

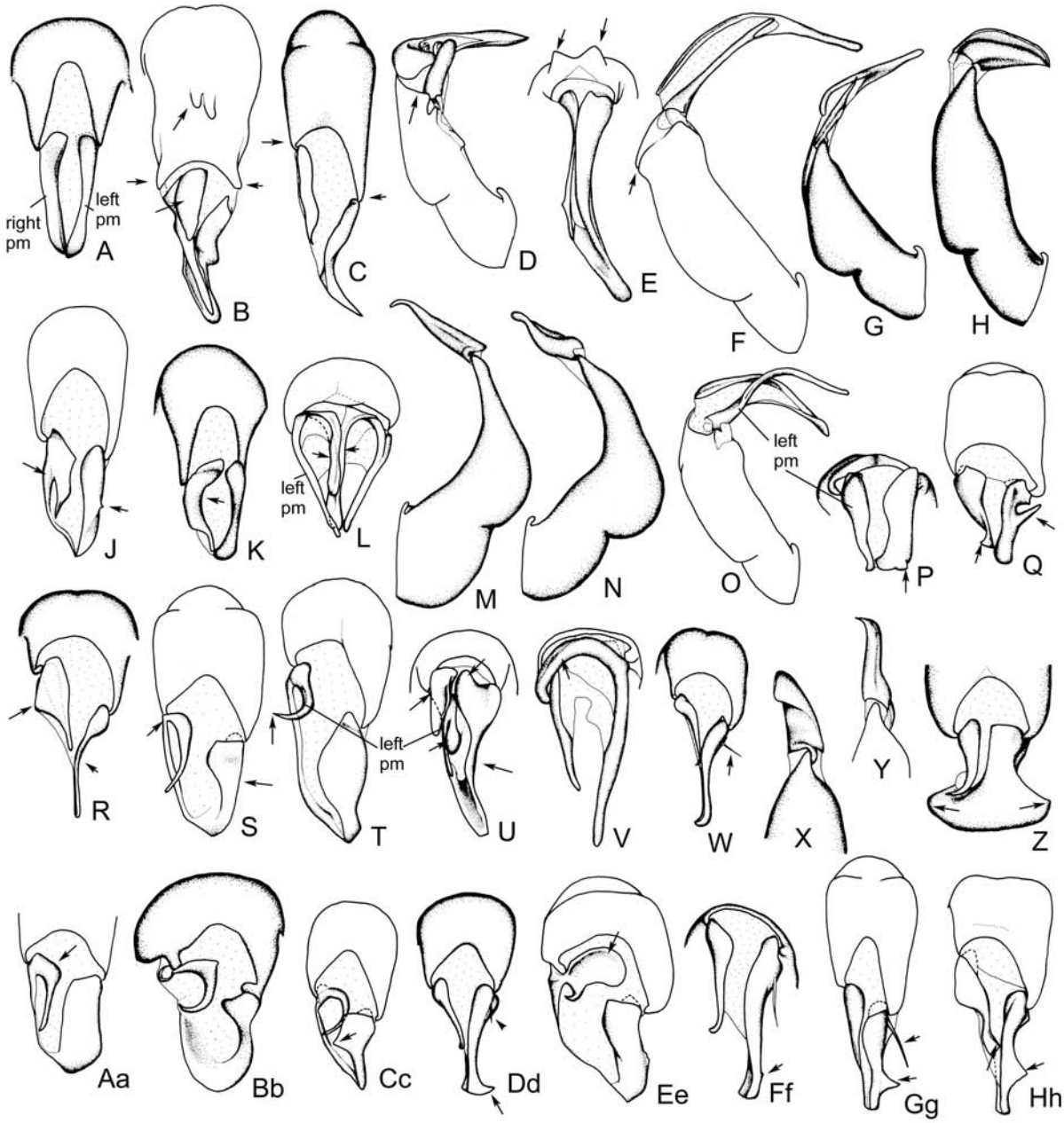


**Fig. 95. A, M:** *Serica karnaliensis*; **B:** *S. hirtella*; **C:** *S. tongluana*; **D:** *S. nanjangana*; **E, F:** *S. bicornis*; **G, R:** *S. thibetana*; **H, P:** *S. kingdoni*; **J:** *S. moupinensis*; **K, N:** *S. erectosetosa*; **L:** *Taiwanoserica anmashanica*; **O:** *S. lijiangensis*; **Q:** *S. mianningensis*; **S:** *S. boops*; **T:** *S. brunna*; **U:** *S. velutina*; **V:** *S. trapezicollis*; **W:** *S. mureensis*; **X, Z:** *S. chasilakhae*; **Y, Aa:** *S. litangensis*; **Bb:** *S. filitarsata*; **Cc:** *S. nipponica*; **Dd:** *S. incognita*; **Ee:** *S. polita*; **Ff:** *S. ribbei*; **Gg:** *S. doiinthanonensis*; **Hh:** *S. lepidula*. **A-C, E, J-L, P-W, Z-Hh:** parameres, dorsal view; **D, F-H, O:** aedeagus, left side lateral view; **M, N:** aedeagus, right side lateral view; **X, Y:** parameres, right side lateral view (not to scale).

90. *Right paramere, lateral preapical tooth*: (0) small and blunt (Figs 95Ee,Ff); (1) large and sharply triangular (Figs 95Q,Gg, 96K,M); (2) very large and long, fork-like produced (Fig. 96B); (3) small, triangularly sharply pointed (Figs 94E,F, 95J, 96O); (4) large and blunt (Fig. 95Hh).
91. *Right paramere, lateral preapical tooth*: (0) before apex of paramere (Figs 95P,Ff,Gg, 96A,C); (1) displaced basally (its position about at middle of the paramere) (Figs 95J,Q, 96O).
92. *Right paramere, dorsomedial margin medially (dorsal view)*: (0) not produced (Figs 95A-C,E,J,K,L,Q-S); (1) bluntly produced (Figs 95T,Bb,Cc,Ee).

93. *Right paramere, blunt dorsomedian extension*: (0) at the middle of paramere (Fig. 95T); (1) in distal half of paramere (Fig. 95Cc); (2) in basal half of paramere (Figs 95Bb,Ee).
94. *Right paramere, lateral/ external margin*: (0) straight (Figs 95A,J,K,L,P,S,V); (1) concavely sinuate (Figs 95B,C,E,Q,R,U,W).
95. *Right paramere, narrow spine on exterior/ lateral face of base*: (0) absent (Figs 94D,F); (1) present (Figs 94G,H,J,N,O, 95W,Ff,Gg).
96. *Right paramere, narrow spine on exterior/ lateral face of base*: (0) very short, shorter than maximal width of ultimate maxillary palpomere (Fig. 94G); (1) long, distinctly longer than maximal width of ultimate maxillary palpomere (Figs 94J, 95W,Ff,Gg); (2) very long, almost half as long as right paramere (Figs 95H,N).
97. *Left paramere, apex*: (0) straight (Figs 95A,B,E,J,L,R,U,Gg); (1) curved inward (Figs 96E,G); (2) curved outward (Figs 94H, 95W,Ee,Ff, 96C); (3) curved dorsally (Fig. 96F).
98. *Ventromedial membrane of right paramere*: (0) membraneous (Figs 95C,G,K,L,R, Bb,Hh, 96P-R); (1) its margin sclerotized from insertion of right paramere to the apex of left paramere (Fig. 95Bb); (2) its margin sclerotized from insertion of right paramere to the base of left paramere (Figs 95J,S,T,Cc,EeAa, 96N,O).
99. *Left paramere*: (0) major part of its surface directed laterally (Figs 96J,K); (1) major part of its surface directed dorsally (Figs 96N,O); (2) surface directed laterally and dorsally in the same proportion (Figs 96L,M).
100. *Left paramere in cross section at basal third*: (0) arched, dorsoventral extension and mediolateral extension equal (Figs 95H,P,Q,Ff-Hh); (1) flattened, mediolateral extension distinctly greater than dorsoventral extension (Figs 95C,G,J,R,S,Z,Aa,Ee); (2) round, dorsoventral extension and mediolateral extension equal (Figs 95T,Bb,Cc).
101. *Left paramere apically*: (0) abruptly pointed (Figs 95A,C,J,K,P,Q); (1) evenly pointed from base (Figs 95S,T,W,Z,Aa-Cc); (2) convexly rounded (Fig. 95D).
102. *Left paramere, at base laterally*: (0) without blunt extension (Figs 95A-C,J-L); (1) with a large blunt extension (Figs 95R, arrow, Hh, 96P,Q).
103. *Left paramere, before apex interiorly*: (0) not widened (Figs 95A,E,P,R-W,Z); (1) bluntly widened (Figs 95C,J, 96O,V,W).
104. *Left paramere, over most of its length*: (0) straight (Figs 95B,C,E,L,P-R); (1) weakly curved outward; (2) strongly curved outward (sickle-shaped) (Figs 95T,Bb,Cc); (3) bent at base and straight (Fig. 95Aa); (4) weakly curved inward (Fig. 95K); (5) bent at base and weakly curved outward (Fig. 95S).
105. *Left paramere, apically*: (0) without elevated lamella (e.g. Figs 95R,S); (1) with a small elevated lamella (Figs 95Hh, 96P).
106. *Left paramere, interior margin basally*: (0) not widened (Figs 95A,C,E,R); (1) lobiform widened (Figs 95B,K,U,Ee); (2) with a narrow basal process (Figs 94K, 95L).
107. *Left paramere, basal process or lobe*: (0) short, distinctly shorter than left paramere (Fig. 94K); (1) long, at least half as long as left paramere (Figs 95L,U,Ee).
108. *Left paramere, its basal lateral margin and the sclerotization of the medial membrane of right paramere* (0) separate (Figs 95R,V,W,Z,Bb,Ff-Hh, 96P-R); (1) fused (Figs 95J,S,T,Aa,Cc,Ee).
109. *Left paramere and medial membrane of right paramere*: (0) shortly fused (at maximum its length half of width of left paramere) (Figs 95Cc, 96S); (1) widely fused (its length equal to the width of left paramere) (Figs 96T,U,V); (2) more than half of left paramere fused with sclerotization of medial membrane (Figs 94L, 95J, 96W).
110. Endophallus: (0) without sclerotized dorsal lobe (Figs 94C,D,G); (1) with sclerotized dorsal lobe (Fig. 94F).

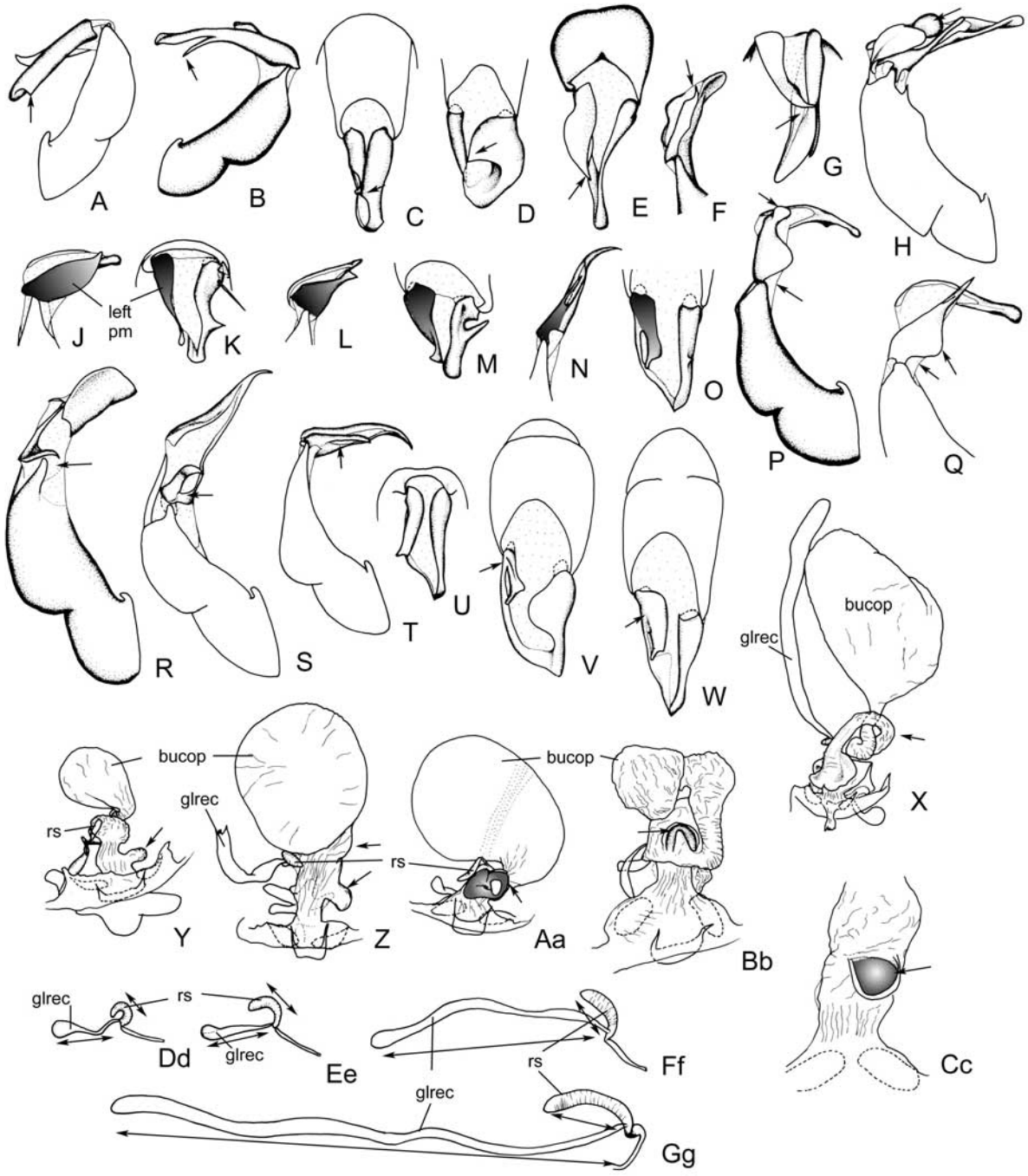


**Fig. 96. A:** *Serica becvari*; **B, G:** *S. kumaonensis*; **C:** *S. ratcliffei*; **D:** *S. montreuili*; **E:** *S. khasiana*; **F:** *S. pommeranzi*; **H:** *S. velutina*; **J, K:** *S. minshanica*; **L, M:** *S. mianningensis*; **N, O:** *S. nigromaculosa*; **P:** *S. lepidula*; **Q:** *S. daliensis*; **R:** *S. filitarsata*; **S:** *S. brunna*; **T, U:** *S. grahami*; **V:** *S. karafutoensis karafutoensis*; **W:** *S. fusifemorata*; **X:** *Pachyserica rubrobasalis*; **Y, Ee:** *S. thibetana*; **Z, Gg:** *P. olafi*; **Aa:** *Lasioserica nobilis*; **Bb:** *S. nigroguttata*; **Cc:** *P. ambiversa*; **Dd:** *S. heydeni*; **Ff:** *S. lijiangensis*. **A, B:** aedeagus, right side lateral view; **C-E, G, K, M, O, U-W:** parameres, dorsal view; **F, J, L, N, Q:** parameres, left side lateral view; H, R-T: aedeagus, left side lateral view; **X-Cc:** female genitalia, dorsal view; **Dd-Gg:** spermatheca (rs) and spermathecal gland (glrec) (not to scale).

*Female genitalia*

111. *Ductus bursae*: (0) short (Fig. 96Y); (1) elongate (Figs 96Z,X,Bb,Cc).
112. *Ductus bursae*: (0) straight (Figs 96Y,Z); (1) coil-shaped winded (Fig. 96X).
113. *Ductus bursae*: (0) not sclerotized, also not partly (Figs 96Y,Z,Bb,Cc); (1) simply partly sclerotized; (Fig. 96Aa) (2) with a sclerotization on left and right side.

114. *Ductus bursae*: (0) without dorsal sacculus; (1) with dorsal membraneous sacculus; (2) with dorsal interiorly sclerotized sacculus.
115. *Spermathecal canal before spermatheca*: (0) not bent (Figs 96Dd-Ff); (1) bent (Fig. 96Gg).
116. *Spermatheca basally*: (0) without sclerotized anellus (Figs 96Dd-Ff); (1) with a sclerotized anellus (Fig. 96Gg).
117. *Spermathecal gland*: (0) much longer than spermatheca (Figs 96Ff,Gg); (1) at maximum three times longer than spermatheca (Figs 96Dd,Ee).

## Results

The analysis of 117 adult characters with the parsimony ratchet and the above mentioned settings repeating the search ten times yielded 167 equally parsimonious trees of 1068 steps (ensemble consistency index (CI): 0.17, ensemble retention index (RI): 0.65). Characters 96 and 116 proved uninformative in the present data set. The tree topology was not affected by altering ACCTRAN or DELTRAN optimizations. The strict consensus of these trees is presented in Fig. 97 with areas of conflict in topology shown as polytomies. The strict consensus tree (Fig. 97) of equally weighted characters exhibits a high level of polytomy, in basal as well as in apical nodes (*Serica*). This is a result of the great number of taxa, of the limited number of characters available for the comparative morphological analysis, and high homoplasy (CI: 0.17).

Four major lineages may be recognized from the strict consensus tree (Fig. 97) within the ingroup: (1) *Calloserica*; (2) *Gastroserica* + *Neoserica*; (3) *Lasioserica*; and (4) *Serica* including the representatives of *Taiwanoserica*. Monophyly of *Pachyserica* was not apparent according to the tree topology. In comparison with the other four principal lineages, the branch support of the node of *Serica* is relatively low (Bremer support: 2, bootstrap value: 56 %). To assume in some manner information of the high number of equally parsimonious trees resulted from the parsimony ratchet with equally weighted characters, a majority rule consensus tree was generated (Fig. 98).

The use of successive approximations character weighting (SACW, Farris 1969) greatly reduced the number of most parsimonious trees (MPTs), producing a significantly more resolved strict consensus tree, especially among the representatives of *Serica*. The shortest trees were found with SACW based on the retention index (ri) (Farris 1989). In this approach weights no longer changed after four iterations (appendix C 3.2.7). From the analysis result six MPTs of 1076 steps (CI: 0.18, RI: 0.69), whose strict consensus tree had the same length (Fig. 99). Although numerous distal nodes are well supported, the bootstrap values for the major nodes are generally low. This reflects the difficulty of finding unambiguous character state apomorphies to support these clades. SACW trees based on consistency index (ci) and rescaled consistency index (rc) were much longer and were abandoned for further discussion.

## Discussion

### *Characters and computer analysis*

The overall structure of the equally weighted majority rule consensus tree (Fig. 98) is the same as in SACW analyses, with the most basal lineages *Calloserica*, *Gastroserica*, *Lasioserica*, and *Neoserica*, and with *Serica* as a monophyletic clade. Many lineages composed of the same taxa, or even numerous identical apical clades may be encountered in both consensus trees. Founded on the retention index (ri) based SACW strict consensus tree

character evolution and evolutionary diversification of *Serica* are discussed. Figures 100 and 101 illustrate the character changes along each branch under DELTRAN optimization.

Morphology of the mouthparts, of the head and of the thorax as well as characters of female genitalia are most consistent with the tree topology of the analyses. These character complexes show more elevated means of consistency index (ci) and retention index (ri). In contrast, characters, such as morphology of the male genitalia and of the legs, frequently applied in species taxonomy of the Sericini, are highly homoplastic, with lowest means of ci and ri (see appendix C 3.2.7).

*Monophyly of Serica and implications on taxonomy and classification*

Although not exhaustive, this study is the most comprehensive phylogenetic analysis of *Serica* ever conducted. The results improve the current understanding of Sericine relationships, as discussed below.

In addition to the four major clades of the strict consensus of analysis with equally weighted characters (Fig. 97) and in contradiction to the majority of its MPTs (Fig. 98), *Pachyserica* proved to be monophyletic after successive weighting based on retention index. It represents the sister group of *Neoserica* + *Gastroserica*, all together resulting the sister group of *Calloserica*.

Being one of the oldest generic names in the tribe of Sericini, most of the older taxonomic works assigned new taxa to the name '*Serica*'. Later, with the description of numerous new genera worldwide, which included a part of the species, formerly assigned to *Serica*, the name *Serica* no longer referred to a monophyletic group, but to a non monophyletic collective group comprising all residual *Serica* taxa. The taxonomic definition of *Serica* thus became more and more ambiguous, also due to a lack of modern revisions. A few authors (Nomura 1972; Ahrens 1999c) made attempts to redefine a monophyletic group with reference to its type species, *Serica brunna* (Linnaeus, 1768). This group was so far explicitly termed '*Serica* sensu stricto' (s. str.) (Ahrens 1999c, 2004b) (see Fig. 99).

Monophyly of *Serica* was evident from present analyses (Figs 97, 99, node A). This node (A) is supported by a number of apomorphies: (1) antennal club in male with three antennomeres (17:1); (2) metafemur ventrally between the two longitudinal rows of setae glabrous or very sparsely setose (41:1); (3) posterior dorsal margin of metafemur serrate (42:1); (4) external lateral margin of protibia bluntly widened medially (47:1); (5) setae of ventral margin of the metatibia fine (52:1); (6) and widely separate (the two apical setae in apical two thirds of metatibia) (53:1); and (7) ductus bursae elongate (111:1).

However, *Serica heydeni* (for whose younger synonym *Podoserica reitteri* Breit, 1912 (synonymized with *Serica* by Ahrens in press c) Breit (1912) established the monotypic genus *Podoserica*), and the taxa of *Taiwanoserica* are nested deeply within the species of *Serica* (arrows, Fig. 99). Consequently both have to be synonymized with *Serica*. For the monotypic *Podoserica* all diagnostic characteristics were identified as autapomorphies. *Taiwanoserica* represents a well supported monophyletic group with species so far described from Taiwan only. *Serica* would have to be considered paraphyletic if the rank of a genus for *Taiwanoserica* is retained.

The subjective synonymy of *Trichoserica* Reitter, 1896 and of *Ophthalmoserica* Brenske, 1897 with *Serica* MacLeay, 1819, established by Nomura (1972), is highly consistent with the tree topologies. The type species of the first (*S. fulvopubens*) is only one node more distal to *S. brunna*, and the type species of the latter genus name (*S. thibetana*) is nested in the same clade (node E, Fig. 99) but slightly more basally to *S. brunna*.

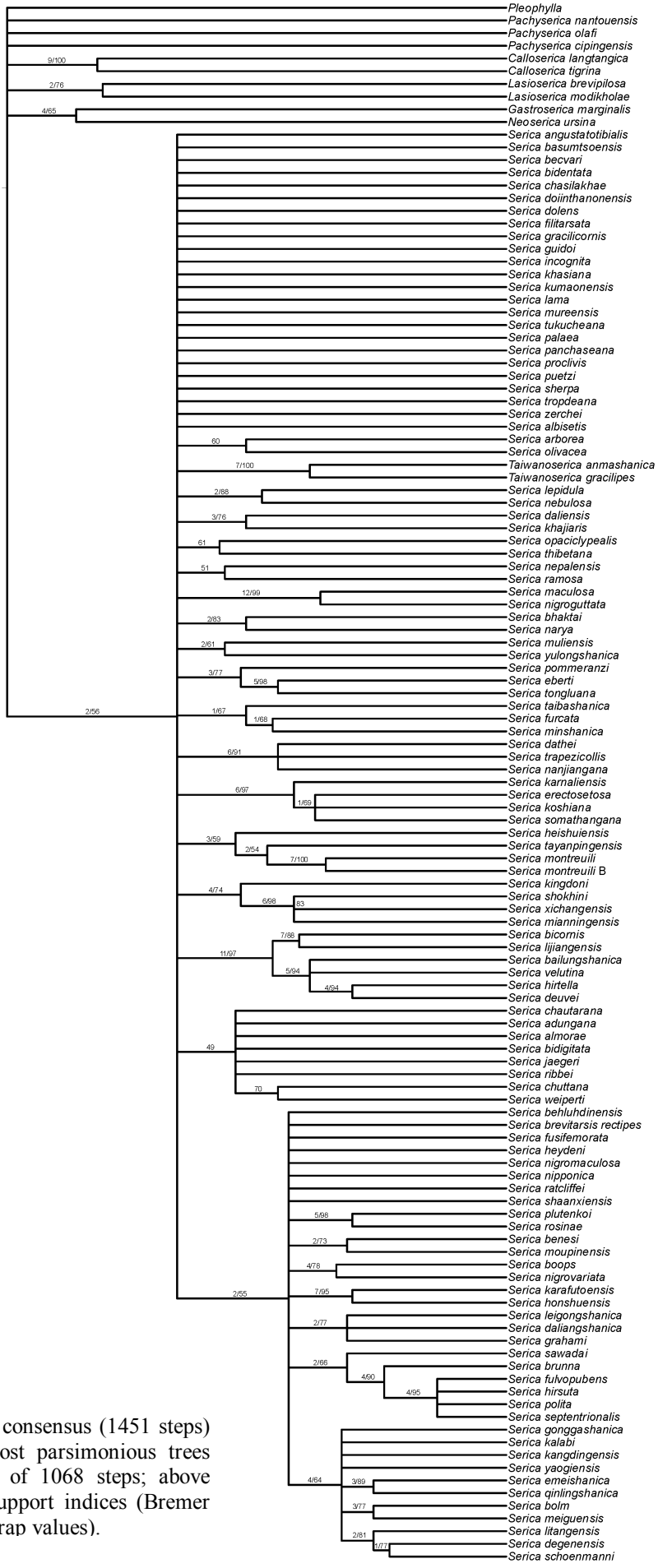


**Fig. 97.** Strict consensus (1451 steps) of the 167 most parsimonious trees with a length of 1068 steps; above each branch support indices (Bremer support/ bootstrap values).


**Fig. 98.** Majority rule consensus (1075 steps, CI: 0.17, RI: 0.64) of the 167 equally parsimonious trees (1068 steps) resulting from parsimony ratchet based on equally weighted characters; above each branch is given the frequency of a node among all MPTs.

The basal *Serica nigroguttata*-group (Fig. 99), represented in these analyses by *S. maculosa* and *S. nigroguttata*, is one of the best supported clades within *Serica*. Many of the synapomorphies of these two taxa included here (Fig. 100), are shared by further 14 species from China, Taiwan and northern Indochina (Ahrens in press a). Some of these have been assigned formerly to *Pachyserica* (Kobayashi and Yu 1993; Ahrens 2002a).

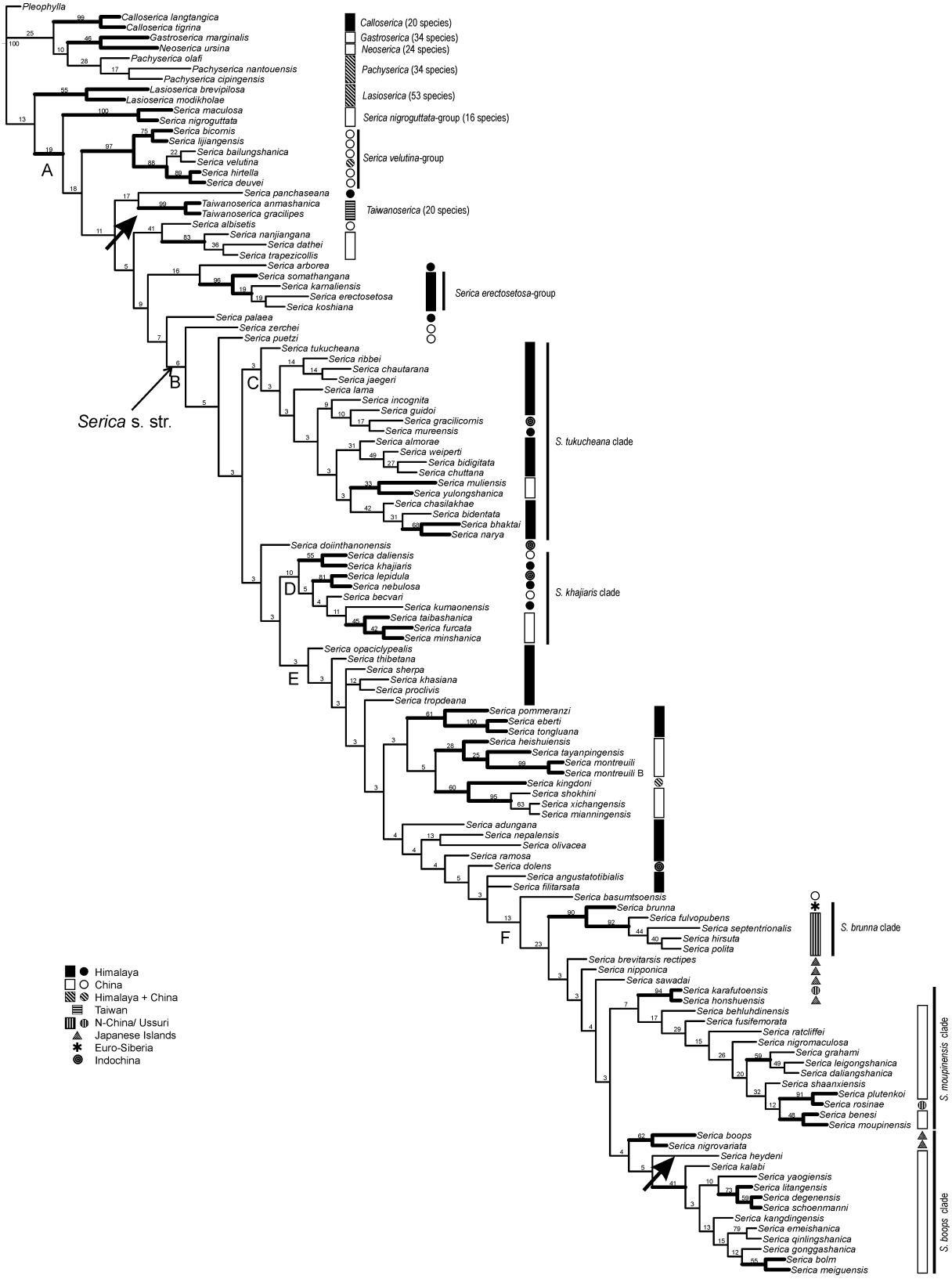


**Fig. 99.** Phylogeny of *Serica*. Strict consensus (1076 steps, CI: 0.18, RI: 0.69) tree of 6 equally parsimonious trees (1076 steps) resulting from successive approximation based on retention index. Above each node branch support (bootstrap value) is indicated. The occurrence of the taxa or lineages is indicated by bands or squares for an ensemble of species or genera, and by an asterisk, filled circle or triangle for single species.

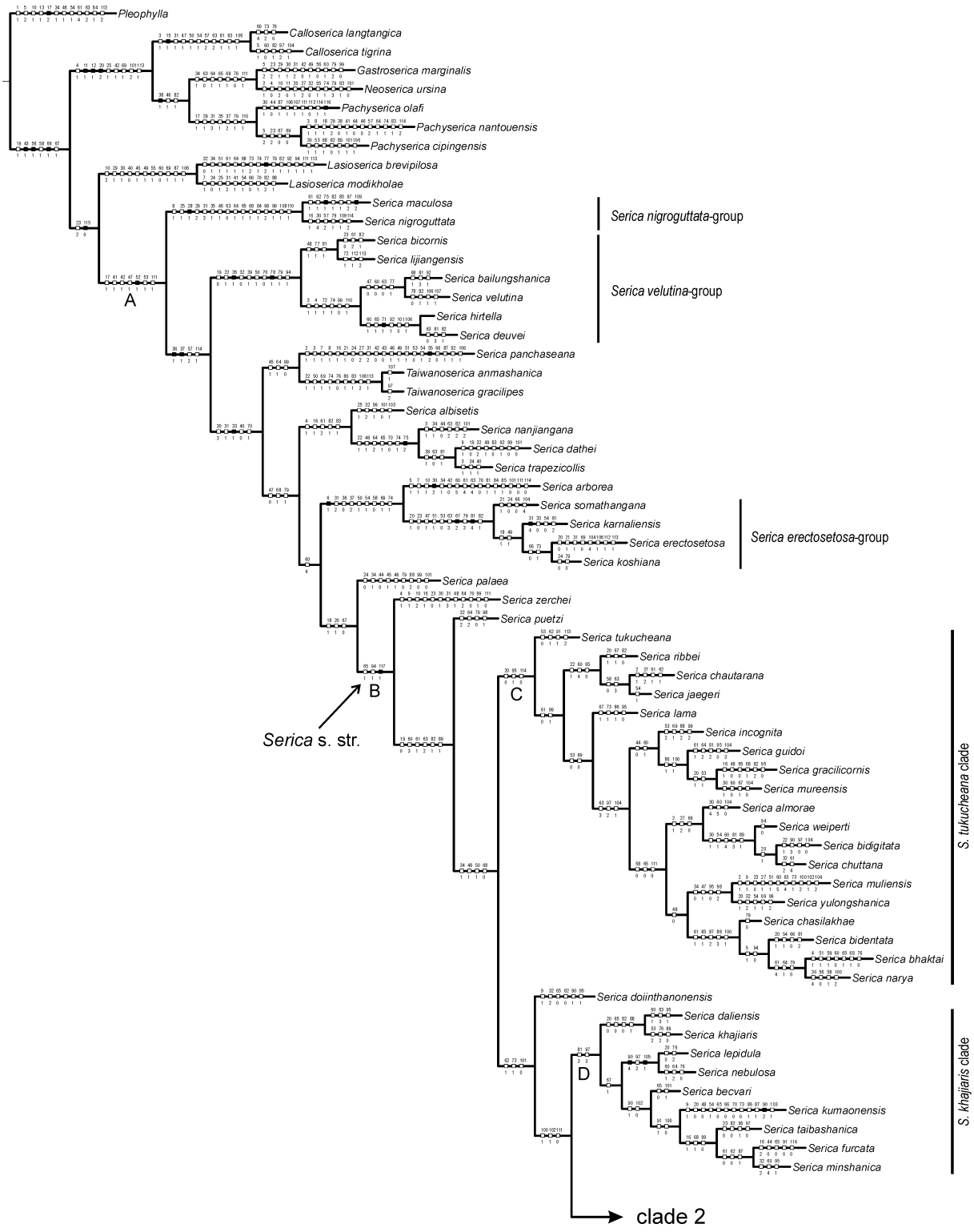


**Fig. 100.** Upper part (clade 1) of strict consensus (1076 steps) tree of six MPTs (1076 steps) resulting from successive approximation based on retention index which shows character changes and apomorphies mapped by state (discontinuous characters are mapped as homoplasy, DELTRAN optimization, unsupported nodes collapsed and using proportional branch lengths) (full squares: non-homoplasious character states; empty squares: homoplasious character states).

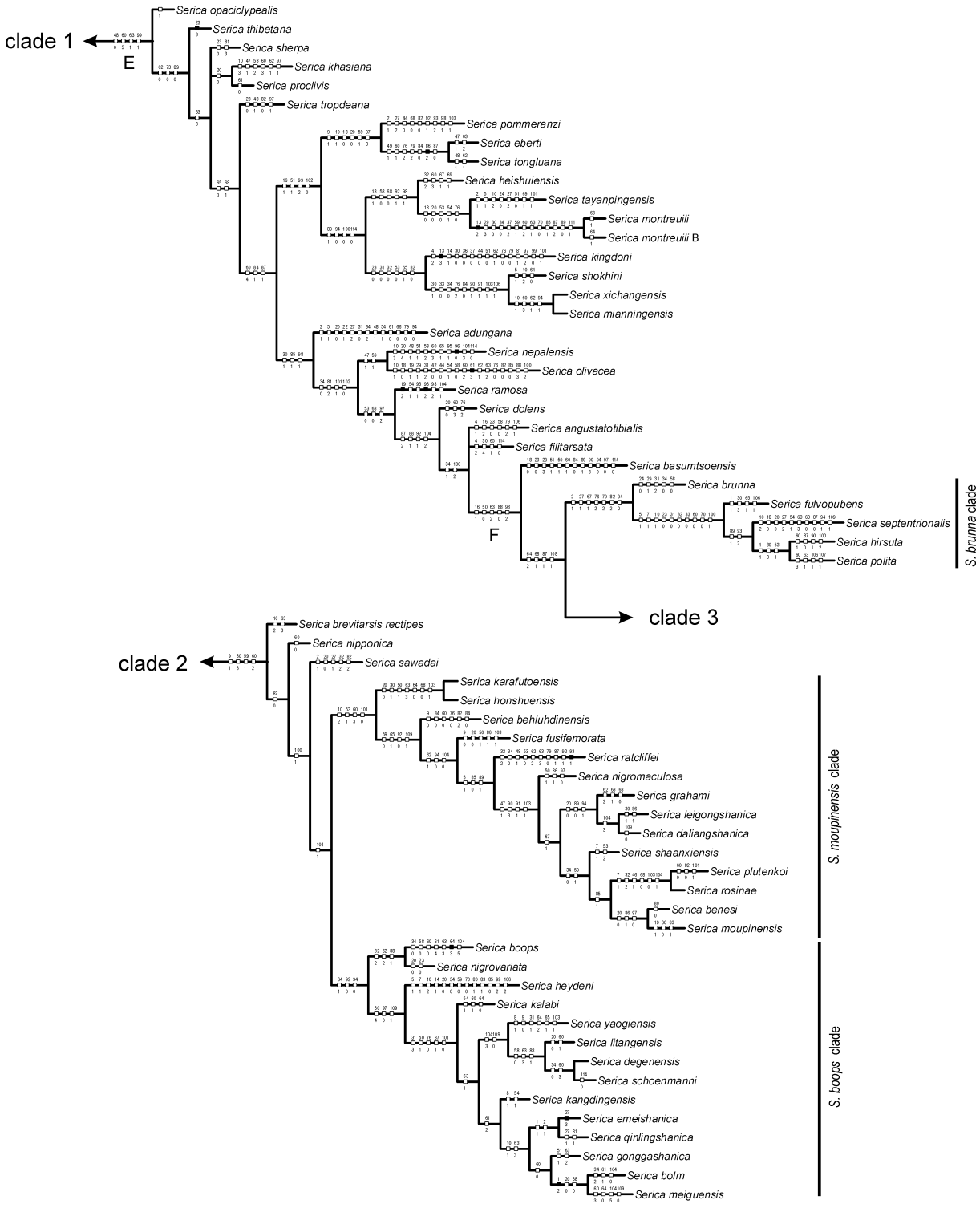


**Fig. 101.** Lower parts (clade 2 (above) and 3 (below)) of strict consensus (1076 steps) tree of six MPTs (1076 steps) resulting from successive approximation based on retention index which shows character changes and apomorphies mapped by state (discontinuous characters are mapped as homoplasy, DELTRAN optimization, unsupported nodes collapsed and using proportional branch lengths) (full squares: non-homoplasious character states; empty squares: homoplasious character states).

## *Evaluation of the clades and evolution of Serica*

A number of well defined principal lineages are apparent in the trees of all analyses. The *Serica nigroguttata*-group discussed already above is one of the most basal showing a very high branch support (Bremer support 12, bootstrap value: 99 %). Subsequently, the *S.*

*velutina*-group represents another well supported lineage of *Serica*. These species occur all in south-western China in the eastern borderland of the Tibetan Highland, with one species, *S. velutina*, penetrating to the eastern Himalaya and Assam. The monophyly of this lineage is founded on several apomorphies (Fig. 100), the strongly and abruptly elevated anterior portion of metasternum (26:1), the laterally impressed metacoxa (39:1), and the dorsoapical phallobase bearing two tubercles (78:1) are the most noteworthy among them. The diverse lineage of *Taiwanoserica* which is here represented exemplarily by two species, is well supported. The parameres subdivided into two long and slender lobes (80:1) is one of its apomorphies being almost unique (ci: 0.5, ri: 0.5). This character state has a similar expression in *S. heydeni* (Fig. 94K). Conversely, a principal diagnostic feature which was used to define *Taiwanoserica* (Nomura 1974), the metafemur possessing a submarginal serrated line beside its anterior margin (45:1), is proved to be plesiomorphic according to results of this analysis. Furthermore, it must supposed that in other lineages, such as *Lasioserica*, a similar structure has evolved resembling strongly this feature. Recently, representatives of this *Taiwanoserica* lineage have been discovered from eastern Tibetan Highland. This discovery raised the questions of whether diversification preceded the arrival of the *Taiwanoserica* lineage on the Taiwanese island, or was the Asian mainland occupied after the diversification on Taiwan ? However, the search for an answer should be addressed to a more detailed study of this lineage including all its known species. The *Serica erectosetosa*-group is another well supported lineage apparent in both analyses with unweighted (Bremer support 6, bootstrap value: 97 %) and weighted characters (bootstrap value: 96 %). As far as it is known this group is restricted to the Central Himalaya, like its hypothesized sister lineage which contains only one species, *S. arborea*.

Subsequently to a monotypic basal lineage (*S. palaea*), a very large clade of *Serica* is apparent. The taxa united in this node (B, Fig. 99) have been grouped presently (Nomura 1972, Ahrens 1999c) under the term *Serica* s. str. (see above). Due to strong morphological homogeneity among the species of *Serica* (and consequently high homoplasy), this node was not evident in the analysis based on unweighted characters, but after successive weighting (node B, Fig. 99). Beside some apomorphies subject to homoplasy, the node is supported by an unique apomorphy, the strongly shortened spermathecal gland (117:1). This character change was, however, reported only under ACCTRAN and DELTRAN optimization mode, since it could not be examined in all species. Some of taxa are known in a very few specimens or in male, only. For this reason, the DELTRAN optimization mode was chosen to display the character changes along each branch. In an obviously successive step, the ventral margin of hypomeron (19:1) was reduced within this lineage. This character state, however, is reversed in a few cases, and apparent in a very similar expression also in the *S. velutina*-group. The ventral margin of the hypomeron has developed within the lineage of ‘modern’ Sericini (chapter 3.1) and is not part of the stem species pattern of the Sericini.

The tree topology is articulated within the *Serica* s. str. clade into several smaller clades, however, due their generally pectinate structure a clear distinction of well separated evolutive lineages is more difficult. As evident from figure 99, basal lineages occur prevailingly in the Himalaya or (western) China, while distal lineages (node F and more subsequent nodes) have occupied in respective manner the Japanese archipelago and the northern parts of East Asia but are completely lacking in the Himalaya, with one species showing even a continuous range extension from Manchuria to western Europe (*S. brunna*).

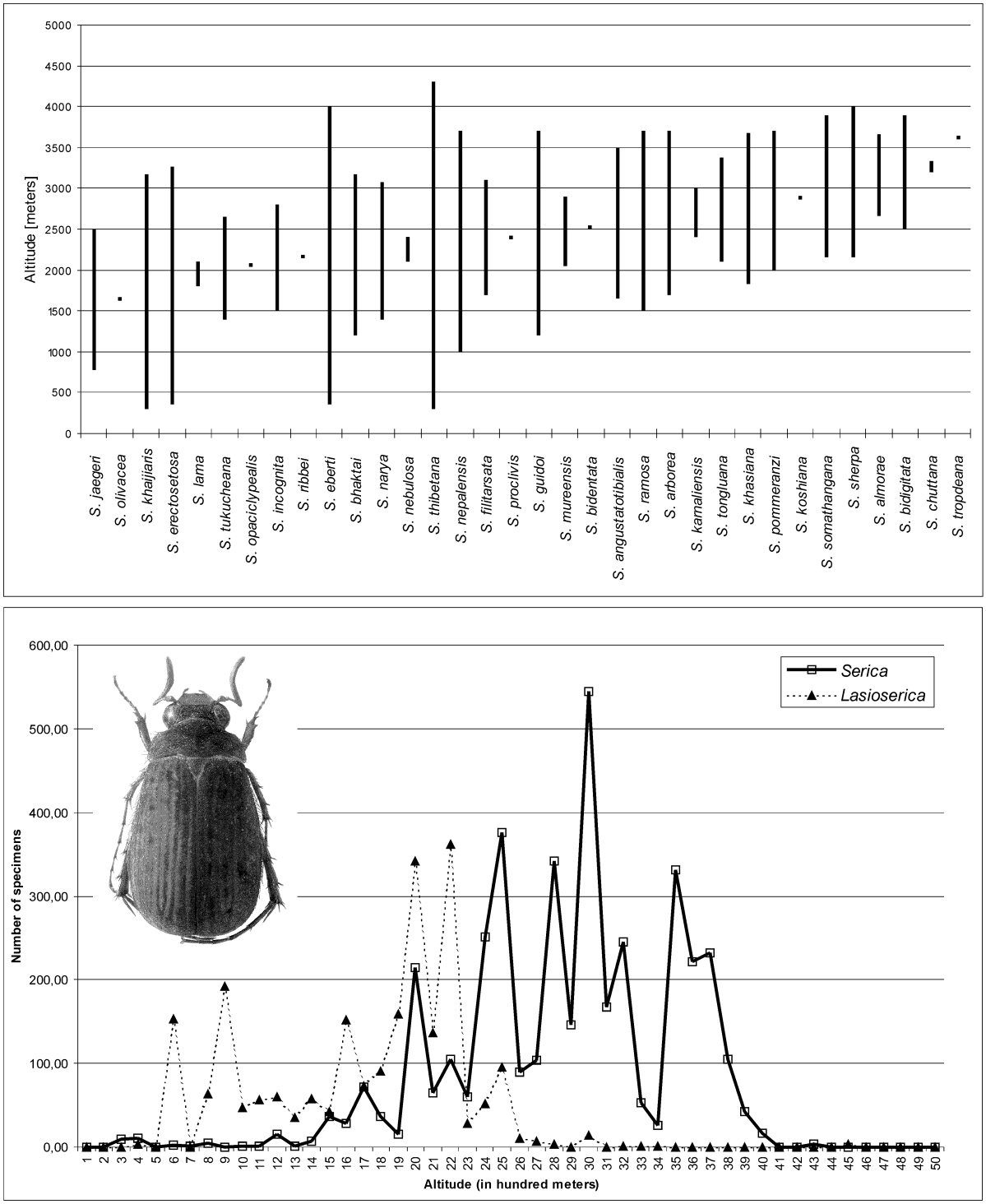


**Figs 102, 103. 102:** Altitudinal distribution of the Himalayan taxa of *Serica* (above). **103:** Total number of records in relation to altitude (in hundred meter steps) cumulated from all Himalayan representatives of *Serica* in comparison to those of *Lasioserica* (below).

Interestingly, among basal lineages the larger clades are not restricted to one geographic region. For example, two species (*S. muliensis* and *S. yulongshanica*) with occurrence in the eastern mountain ranges of the Tibetan Plateau are nested among the taxa of the *S. tukucheana* clade (node C) with almost exclusively Himalayan distribution. Similarly, in the *S. khajiaris* clade (node D), Himalayan (*) and eastern Tibetan taxa establish closest relationships, as in the sister groups *S. daliensis* + *S. khajiaris** or *S. gracilicornis* + *S. mureensis** (Indochinese and Himalayan), or as in the clade *S. becvari* (*S. kumaonensis** (*S.

*taibashanica* (*S. furcata* + *S. minshanica*))). In other words, although the Himalaya being well defined geographically, the taxa occurring there do not form a single major monophyletic lineage. Such a pattern is as far as known particular among Himalayan Sericini being part of the fauna of the montane altitudinal zone. Other montane groups, such as *Lasioserica* or *Maladera* (subgenus *Omaladera*) are restricted to the Himalaya also in major clades (Ahrens unpl.).

In contrast to the species of these groups, the occurrence of the taxa of *Serica* is predominant at higher elevations, as evident from a comparison of the Himalayan taxa with those of *Lasioserica* (Figs 102, 103). However, this would be strong evidence to assume that flight-active organisms of medium and upper montane belt had or have better opportunities for dispersal along and across higher mountain chains as encountered in the Himalaya or eastern Tibet. In fact, among these forms of the medium and upper montane belt we encounter vast ranges such as in *Serica thibetana*, whose range extends almost continuously from northern Pakistan to Yunnan (China), and for which the highest altitudinal extension (up to 4300 meters) has been recorded.

Probably, the taxa capable of flight, are enabled during warmer and drier periods to cross higher passes and ranges, when the snow line is elevated, reaching adjacent valleys or even the Tibetan Plateau, where they have met along the Yangtze suitable conditions for a long distance-dispersal. This hypothesis is supported by evidence, that Tibet very probably has never been completely covered by a large ice sheet (Schäfer et al. 2002). That these hypothesized dispersals with subsequent separation might be one of the principal processes responsible for speciation and consequently the high diversity of the Himalayan - East Tibetan mountain ranges, becomes evident from some of the present distribution ranges of Himalayan *Serica*. Ranges of *Serica eberti* and *S. tongluana*, which result from cladistic analysis to be sister taxa, are parapatric. However, the range of *S. tongluana* is enclosed at the southern slope of the Himalaya between the eastern and western part of the range of *S. eberti* (Fig. 104). This pattern can be explained only in the framework of the morphospecies concept and under the most parsimonious assumption, hypothesizing for *S. eberti* a formerly continuous range north of the main Himalayan chain while *S. tongluana* has been restricted to the southern slope of the Himalaya.

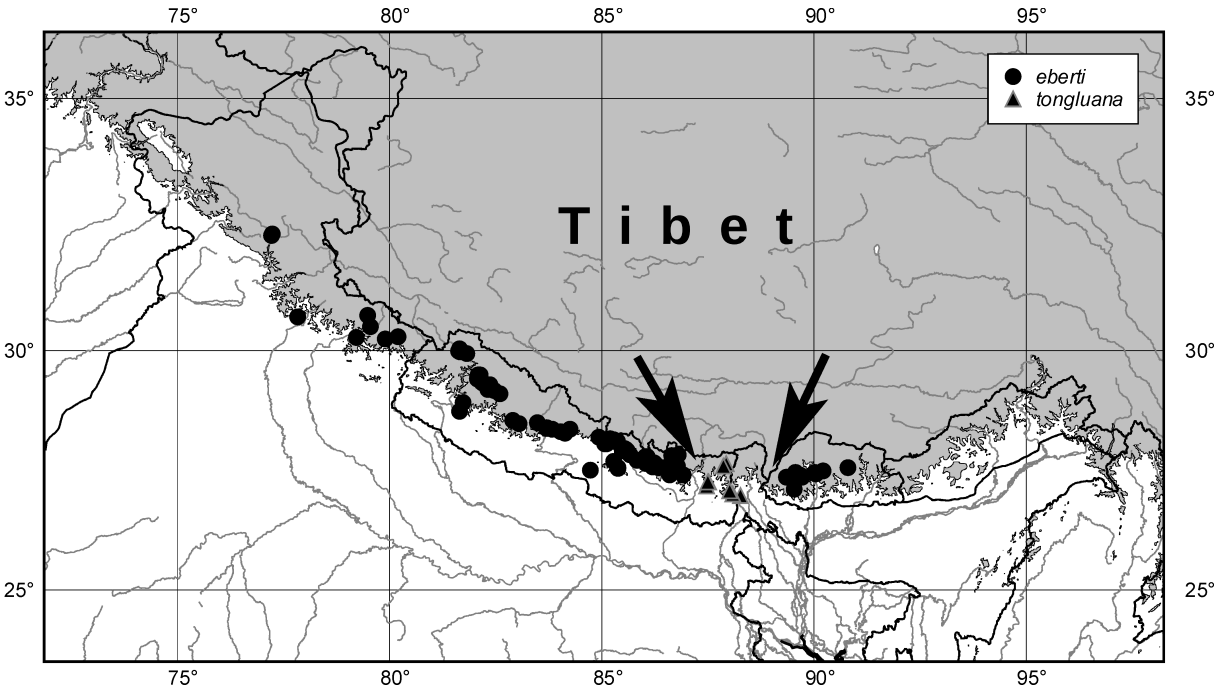


**Fig. 104.** Distribution of the sister taxa, *Serica eberti* and *S. tongluana*. Areas above 2000 meters are grey shaded. The range disjunction of *S. eberti* is indicated by arrows.

Although not all Japanese species of *Serica* could be included in the analysis, some obvious patterns are recognizable from the topology of the distal *Serica* clades. The most distal lineages subdivided principally into three distinct clades: (1) the well supported *S. brunna* clade, evident from all analyses; (2) the *S. moupinensis* clade; and (3) the *S. boops* clade. The first is exclusively distributed on the north Asian mainland, the two latter clades have basal lineages occurring on Japanese islands, while the more distal taxa are distributed in northern and western China (Fig. 105). The *S. moupinensis* clade and the *S. boops* clade result as sister taxa according to the topology of the ASCW strict consensus tree. Since the taxa of three basal lineages to *S. moupinensis* clade + *S. boops* clade are all Japanese forms, it must supposed that for the diversification of these two clades the Japanese islands were of a certain importance, but also the feasible faunal exchange to the Asian mainland. The northward shift of the ranges of the distal lineages and the diversification of these clades on the more humid Japanese islands with their high mountain ranges (Fig. 105), however, must be debated considering also the climatic deterioration in northern Asia during late Tertiary. Associated with the onset of the monsoon since 8 Ma (Ruddiman and Kutzbach 1989) as well as with the aridization (Guo et al. 2002) in consequence of the retreat of the Paratethys (Ramstein et al. 1997), climatic contrasts have strengthened since this period.

The taxa of the *S. moupinensis* clade + *S. boops* clade are absent in the Himalaya. This might be attributed to the fact, that they could have occupied the eastern Tibetan mountains rather late. With the advancing uplift of southern and central Tibet as well as of the Yunnan Plateau and later also of the north-eastern Tibetan Plateau, these highlands became an effective geographical divide for the taxa of these lineages. Only a few species or lineages (e.g. *S. bolm*, or the stem species of (*S. litangensis* (*S. schoenmanni* + *S. degenensis*)) (*S. boops* clade) could (partly) cross or occupy these highlands.

Dispersal leading to the disjunction of the sister taxa *S. daliensis* + *S. khajiaris*, *S. nebulosa* + *S. lepidula*, and *S. gracilicornis* + *S. mureensis* (Fig. 106) has presumably taken place along the southern margin of the ranges of the Himalaya, Tibet, and Yunnan. The widely disjunct ranges of the taxa of the basal lineages such as *S. palaea*, *S. zerchei*, *S. puetzi*, those of the taxa of the *S. tukucheana*- / *S. khajiaris* clade, as well as the widely separated ranges of the most basal *Serica* lineages, lead to the assumption that the interfering area between the Himalaya and eastern Tibetan mountain ranges, namely the formerly less elevated Tibetan Plateau, was in the past easy to traverse for flight-capable organisms adapted to a cold-temperate climate. Although data of this analysis provide no evidence for such an assumption, and also fossils or molecular data are lacking, the hypothesis may not be excluded that these formerly less elevated highlands were even a region with very suitable conditions to stem lineage representatives of present *Serica* clades, from where the stem species of these lineages have occupied the Himalaya and/ or eastern Tibetan ranges.

Such a hypothesis would be highly consistent with the evidence from geological data, indicating a high age of the southern Tibet Plateau (Tapponnier et al. 2001) as well as an early presence (30 Ma) of relatively high mountain ranges (Himalaya ~ 1 km, Gangdese Shan 3 ±1 km) at the southern margin of the Asian continental plate (Harrison et al. 1998). Based on their studies of well preserved fossil leaf assemblages from the Namling basin, southern Tibet, Spicer et al. (2003) concluded that the elevation of the southern Tibetan plateau probably has remained unchanged for the past 15 Ma. However, Tapponnier et al. (2001) reveal also, that the great extension of Tibetan Plateau was achieved rather late during Miocene/ Pliocene, when north-eastern parts of Tibet were significantly uplifted.

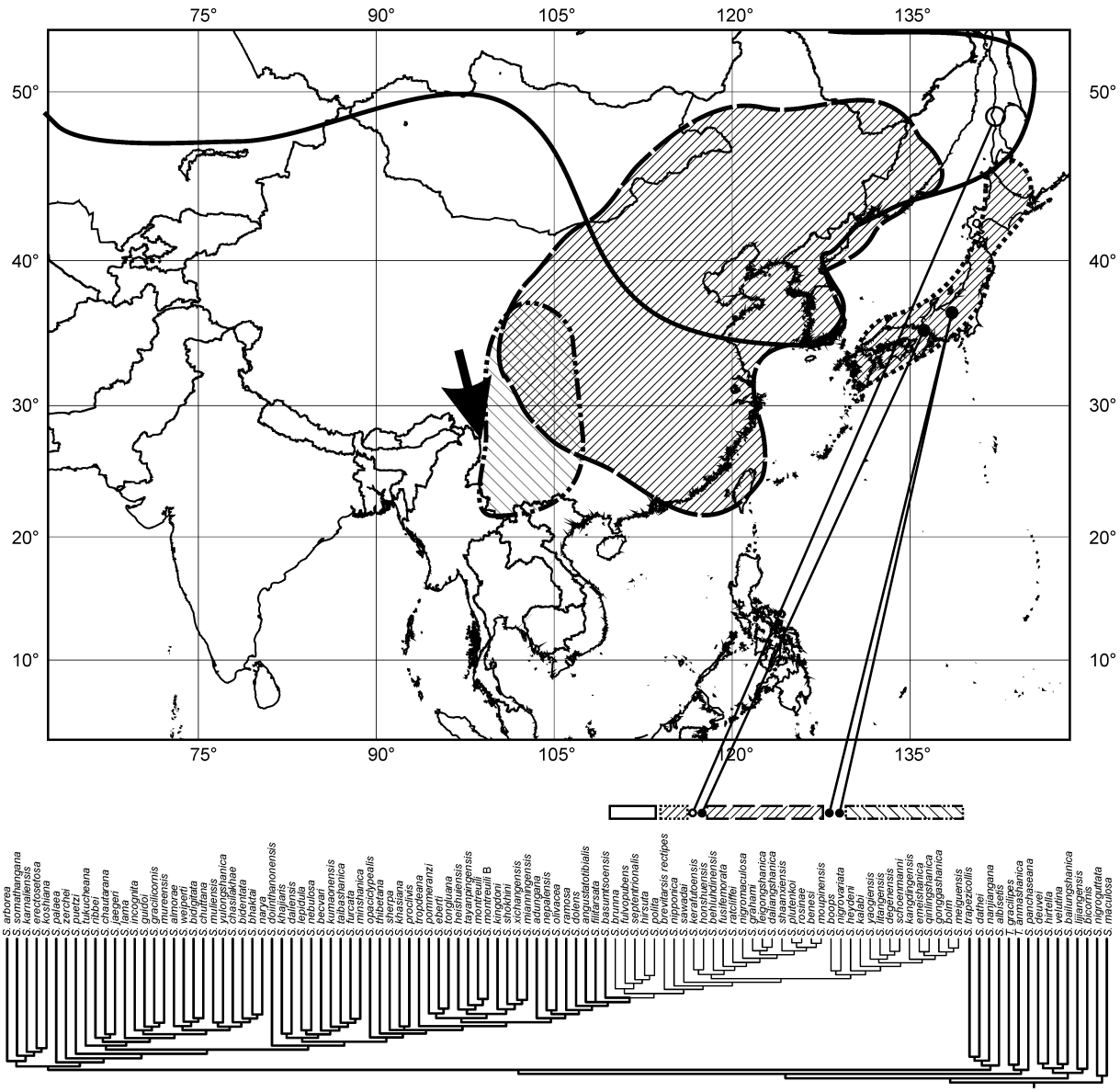


**Fig. 105.** Phylogeny of *Serica* in its geographical framework, with indicated cumulative generalized distribution of the more distal lineages (indicated by narrow branch lines) and some of its species, namely the *S. brunna* clade (range: continuous line), the *S. moupinensis* clade (range: shaded narrowly), and the *S. boops* clade (range: shaded widely in the other direction). The taxa of these lineages were not able to cross the Tibetan/ Yunnan Plateau and to occupy the Himalaya due to the barrier effect of the more and more uplifted eastern Tibet and Yunnan Plateau.

The apical lineages assigned so far to the clade *Serica* (s. str.) are obviously absent from lowlands of southern and eastern China. Thus, the occurrence in elevated altitude of Taiwan with one species, *S. fusifemorata*, is widely isolated. Since almost all taxa of *Serica* (s. str.) clades prefer elevated mountainous (in lower latitude) or temperate habitats (in higher latitude), a dispersal from Asiatic mainland to Taiwan must have coincided with a period of climatic deterioration, as occurred during the Pleistocene, when Taiwan had a land connection with the remainder of Asian mainland.

The results presented here, although beginning to reveal an overall phylogenetic framework for *Serica* that is relatively robust, as well as suggesting a number of well supported species relationships, are still very far from satisfactory regarding their completeness and the capacity to generate data with a temporal dimension, as for example is provided by molecular studies. Within all Sericini examined in the course of these studies, the extreme homogeneity in adult morphology left a great part of deeper nodes, especially those

connected with basal lineages or generic relationships, poorly supported. For many taxa, only a small number of specimens were available for examination, often known in one sex only. Although several regions are still relatively unexplored faunisticly, the present analysis revealed so far interesting patterns of beetle evolution in Asian mountainous regions and highlands being, hopefully, an impulse for further investigations and explorations in the future.

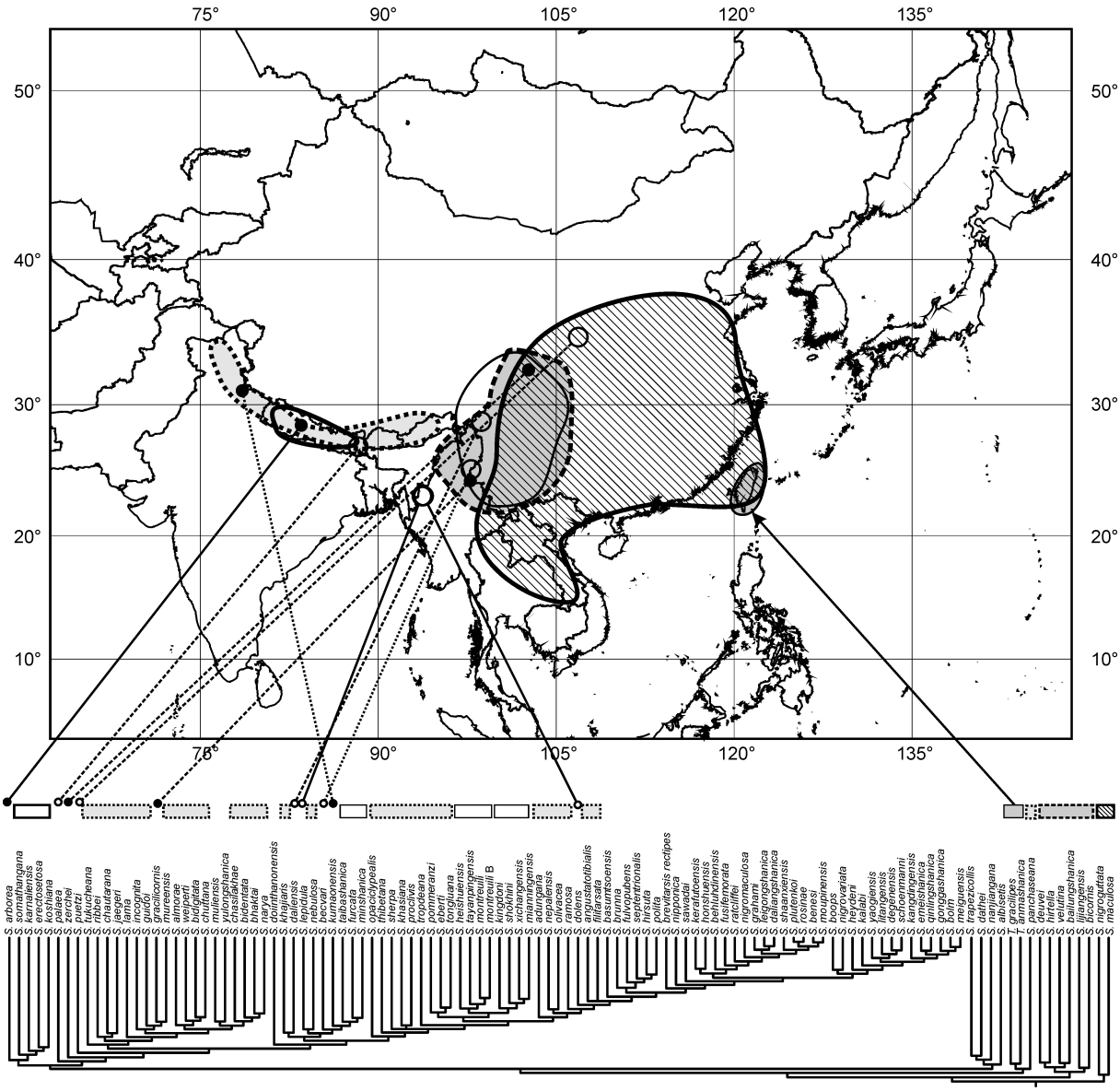


**Fig. 106.** Phylogeny of *Serica* in its geographical framework, with indicated cumulative generalized distribution of the more 'basal' lineages. Ancestral species of these lineages were able to cross the formerly less elevated Tibetan/ Yunnan Plateau and to occupy the adjacent mountain ranges. More closely related taxa are supposed to have dispersed prevailingly along the southern slopes of the Highlands.